

Reply to the reviewers

Anonymous Referee #1

This is a useful technical paper describing an advancement in the way that simulations of ice crystal growth in the laboratory are performed. A lot of work has gone into this chamber, and I'm happy to see all the considerations & analysis published so others can use it and understand the strengths and weaknesses of the technique.

I recommend publication, following some minor corrections.

Our Reply: We thank the reviewer for their helpful suggestions. We point out here the changes made to the revised manuscript:

Introduction "but each experiment seems to give different normal growth rates (i.e., rate of face advancement normal to itself), even under similar conditions and using similar techniques" - can you provide examples of this, and relevant citations here?

Our reply: We followed the reviewer's suggestion and have added citations to the data sets showing the large variations at -15C and -30C.

I felt section 2 was a very long unbroken section. It would benefit from being broken up a bit - for example splitting into subsections and including more of a "road map" at the start of the section outlining the issues to be addressed

Our reply. We have added new subsection headings in bold to increase the readability of this section.

Equation 1 - I'd say ρ is more conventional notation for density . . . The analysis that follows could be spelled out more clearly. Why is the numerator proportional to dT ?

Our Reply: Equation 1 is a standard definition of supersaturation. N is the common symbol for number density in the crystal-growth literature. We prefer the symbol N to avoid confusion as the symbol ρ is used for the mass density of the air and vapor. Also ρ is the usual symbol for the mass density of water and ice, ρ_w and ρ_i , respectively. The numerator is

equilibrium number density difference between the vapor source temperature and the surface temperature. We have rewritten this section of the paper to add clarification to the text.

You do a “back of the envelope” calculation here, with the Hertz-Knudsen equation - what assumptions does this calc make? e.g. regarding crystal + growth kinetics.

Our Reply: The estimate was made with the assumption of $\alpha = 1$. We have added a reference to the Hertz-Knudsen equation to the text.

"If we assume that the onset of convection occurs with a Rayleigh number of about 1500, . . ." more background needed. can you justify this threshold, and define Ra physically

Our Reply: We have estimated the Rayleigh number for the onset of natural convection. We have referenced an experimental and numerical study showing approximately this value for convective onset and have added a little more explanation to the text.

Page 5, last paragraph. Up to this point the analysis seems to suggest that S_a can be estimated very precisely. But reading this last paragraph, I wasn't sure what to think. The author's conclusion needs to be more explicit here. You say the computed S_a in your “other experiments” was different to the real value (using droplet as a reference for the environmental saturation ratio). Can you be quantitative? How different? More than you would expect from the preceding estimates? If so, why might this be? And what is the implication for analysis of results from the chamber generally?

Our Reply: We have rewritten this section to explain more clearly the limits to S_a determination. The “gold standard” for crystal growth experiments is stable T and S conditions in a chamber along with direct measurements of S and T near the crystal surface simultaneous with the growth rate measurements. To date there have been no experiments with a direct measurement of S near the crystal surface simultaneous with the growth rate measurements. We have made droplet evaporation measurements simultaneous with crystal growth measurements to obtain a direct measurement of S_a . But precise determination of S_a is not required here as we are focusing on the differences in facet-normal growth rates for crystals growing simultaneously in the chamber under the same growth conditions. We have added the estimated value of S_a using Eq. 1 to the text. Unfortunately there isn't space here for describing in detail our new method for more precise S_a determination and this will be reported elsewhere.

Response to Referee #2

The manuscript by Swanson and Nelson describes a steady state diffusion chamber designed for high-precision studies of ice crystal growth and sublimation. It appears to be a companion paper to the study of the formation of air pockets in growing ice crystals (Nelson and Swanson 2019) which has been conducted with the apparatus described here. The manuscript presents a very thorough description of the apparatus and discuss deeply the principles of operation and potential error sources. The images of the ice crystals grown with the help of the apparatus are amazing and obviously demonstrate the ability of the system to maintain stable temperature conditions for a very long time.

Our reply. We thank the reviewer for their careful review. The reviewer has several concerns and we have rewritten the sublimation section of the paper to clarify how we determine S_a and we have included the S_a estimate in the text for the Section 3 result.

The manuscript, however, provides no convincing evidence that the apparatus can be used for studying diffusion growth of ice crystals under *predictably controlled* supersaturation conditions. By that I mean that in order to understand and to describe the crystal growth, the water vapor pressure in the vicinity of the crystal has to be set to and precisely maintained at the *predefined* value, which can be either derived from the instrumental parameters or obtained via calibration. This ability has not been demonstrated in the manuscript. Instead, there is a lot of discussion of the potential errors and why they should have negligible effect on the growth rate of the crystal.

Our reply. We have rewritten this section of the manuscript to clarify how S_{VS} is determined. We hadn't realized the interest in the estimated S_a for simultaneous growth experiment but we now have provided the estimated S_a for the results presented here.

It seems that the previous version led to some confusion. Our chamber is not a diffusion chamber. Hallett and Mason used a diffusion chamber, as did Bailey and Hallett. Ours is a different design. The sliding valve seals one VS or the other from the GC during operation. So only one of the two VS is setting S_{gc} . In our chamber the supersaturation is set by T_{vs} and T_{gc} and is given by Eq. 1. This is the same method of setting S_{gc} used in numerous other studies such as the Gonda 1983 and 1994 studies. But the thermal control in CC2 is much improved compared with previous methods. Gonda 1982 and most other previous experiments do not report the size of their spatial and temporal temperature fluctuations whereas the CC2 design specifically minimizes these gradients.

What I am desperately missing is the characterization of the instrument in terms of supersaturation as a function of a) temperature of the growth chamber, b) temperature of the both vapor sources, c) spatial coordinate in the growth chamber, d) time. As authors themselves put it: *"We conclude that accurately predicting and maintaining a constant S_a at a chamber center without a direct measurement of the supersaturation requires careful calibration"* (page 5 line 34-35), but the calibration is missing. In fact, in the whole manuscript, not a single value of the supersaturation (or vapor pressure) in the growth chamber is given. The closest occasion where the word "supersaturation" is used in conjunction with any numerical values is *"During part A S_a was not highly controlled but conditions were maintained such that $-0.5\% < S_a < 0.5\%$. During part B S_a was controlled such that $T_{VS} = -29.3 \pm 0.4 \text{ }^{\circ}\text{C}$ "* (page 8 lines 30-31). How this value of S_a has been deduced? Why were the crystals growing if the supersaturation was zero on average?

Our reply. CC2 is designed for experiments observing multiple crystals growing simultaneously on tiny capillaries all within about a 1 cc volume at the center of the EC. The temperature stability of the EC has been measured to be less than 50 mK over a 1 day period. The temperature gradient across the 13 x 7.5 x 20 cm EC is on order of 10 mK over a 11 hour period. So to first-order the supersaturation gradient across this volume is given approximately by $\delta S \approx (\delta T/T) * S$ which is negligibly small. Therefore S_{vs} can be estimated using Eq. 1 as stated in the manuscript on P. 4-7.

The paper shows several examples of the high-resolution imaging possible in the CC2 and detailed measurements of crystal size can be made using these images. In the Snomax nucleated crystal experiment (results shown in Figs. 5 and 6) multiple crystals were growing *simultaneously* on the capillaries all within about a 1 cc volume at the center of the EC. These results are showing the crystal shape differences as a result of simultaneous growth with all crystals experiencing the same supersaturation. We conclude supersaturation differences are not responsible for the differences observed here. The facet normal growth rate and shape differences are instead likely due to different growth processes occurring at the different facet surfaces. This is a small result but seemingly not well appreciated in previous experiments due to possibility of changing growth conditions surrounding the crystals of interest. S_{vs} for the experiment is reported near the bottom of P. 9.

The explanation why the actual supersaturation cannot be derived from the temperature of VS is offered on page 6, starting from line 1: *"In a highly controlled vapor-source supersaturation, S_{VS} , does not necessarily set the*

ambient supersaturation, S_a , at the center of the chamber where the crystals are growing if there is unobserved condensate growing on the wall." The issue is being addressed by observing the chamber surfaces visually, with the remark "*But it is possible that this ice is so thin as to make it nearly invisible to the eye*" (page 6 lines 6-7) . I don't see how one can control AND measure the actual supersaturation under these conditions.

Our Reply: Previous experiments have simply estimated the growth temperature and supersaturation conditions in various chambers without detailed calibrations or actual measurements. No previous ice crystal growth experiment has actually measured the temperature and supersaturation near the surface of the growing or sublimating crystal. Such a result in itself would be a major breakthrough for crystal growth technology and the report of such an accomplishment is not our claim here. Instead we expect S_{vs} is well approximated by Eq. 1 and deviations are due primarily to the temporal and spatial gradients in the growth chamber and vapor source chamber temperatures. These gradients are described in detail in section 2.

For this report higher-precision determination of S_{gc} is not required as this is a simultaneous growth experiment. We will be demonstrating how we can use droplet evaporation measurements simultaneous with growth rate measurements to check the chamber supersaturation in a future publication.

Now, the authors claim that "...*typically no frost was observed on VSC walls for at least 6 hours*" (page 6 line 20). In this case the question arises, how it was possible to conduct an experiment for 92 hours as described in the section 3? Obviously, this would require multiple de-icing steps as described on page 6, lines 18-19, during which the GC has to be disconnected from the VSC and reconnected to the second VSC with the VS set exactly to the same temperature. Or was the GC just left connected to the VSCs resulting in no supersaturation, as implied by the sentence "*During part A S_a was not highly controlled but conditions were maintained such that $-0.5\% < S_a < 0.5\%$.*"?

Our Reply: For these long-period growth experiments frost would sometimes form on VSC walls but none was observed not on the GC walls (if frost were to appear on GC walls then experiments would be terminated and these walls cleaned before a new experiment could start). CC2 is designed so that if one VSC does start to grow frost then the sliding valve can be set in the opposite position to isolating this VSC from the GC. With the valve in this new position the GC would be now experiencing vapor from a clean-walled 2nd VSC with its TEC set to the same VS temperature. To remove frost off from a VSC wall we reduce the TEC temperature and pump out the chamber until the walls were clear of ice. Now this newly clean-walled VSC is ready for use if frost were to form on the other VSC walls.

If the setup was build to study the ice crystal growth at atmospherically relevant conditions, it should be possible to set and maintain supersaturations up to 30%. Nothing in this manuscript tells me that this is feasible.

Our Reply: CC2 is designed to maintain much higher supersaturations than the experiments described here. At larger S_a we observe significantly larger growth rates. But this paper's focus is on the improved imaging capabilities and temperature stability of the instrument. The report of data sets made at different T conditions and at higher S_a will come later. The goal of the experiments reported here was not to explore the full range of T and S conditions but instead explore the differences in facet normal growth rates for crystals growing under the same conditions.

If calculation of the supersaturation based on the instrumental parameters is not possible, a calibration can be achieved by measuring diffusion growth or evaporation of a reference particle – droplet of a known solution. Apparently, the authors have done that: “...we have in addition used droplet evaporation measurements done simultaneously with crystal growth measurements to give a direct, and independent, estimate of S_a ” (page 5 line 30). It’s disappointing that this direct and independent estimate of the supersaturation is neither given nor discussed further. The only measurements of the crystal growth rate presented in the manuscript (Figure 6) are not compared with any other measurements or with theory; we learn that the growth rate can be fitted by a two-parameter power- law parameterization, but no further attempt of interpretation is given. Actually, even the fit parameters are not given or discussed, and the reader is informed “A more detail discussion of these results is reported elsewhere” leading to a reference (Swanson 2019a) that has a different title and dedicated to a different topic (I assume this is the reference to the paper in ACPD by the same authors. Actually, the reference to Swanson 2019b leads to nowhere). I have not been able to find any discussion of these results in the companion paper.

I am afraid I cannot recommend publishing the paper in its present form. It should be thoroughly revised aiming at providing a verifiable characterization of the apparatus under wide range of experimental conditions. If the supersaturation cannot be calculated from the instrumental parameters, it should be calibrated in a dedicated experiment with evaporation or condensation of inorganic solution droplet, and the results reported together with the theoretical model used for the simulations. I am not in a position to give advice on the chamber design, but perhaps it would be better to create well-defined wall boundary conditions in the VSC and CG chambers by covering walls with ice than relying on the absence of water adsorbed on the bare metal walls of the chamber.

1. Nelson, J. and B. Swanson (2019). "Air pockets and secondary habits in ice from lateral-type growth."

Atmos. Chem. Phys. Discuss. **2019**: 1-51 doi: 10.5194/acp-2019-280.

Our Reply: As we mentioned above, we have rewritten this section to explain more clearly the limits to S_a determination. For the Snomax crystal experiments S_{vs} is now reported at the bottom of P. 9. To date there have been no experiments with a direct measurement of S near the crystal surface simultaneous with the growth rate measurements but we have made droplet evaporation measurements simultaneous with crystal growth measurements to obtain a direct measurement of S_a . But these measurements were not done during the Snomax crystal growth experiments as a more precise determination of S_a is not required here. Crystals were grown simultaneously under the same thermodynamic conditions to observe differences in facet-normal growth rates under the same growth conditions. In future experiments when sequential measurements are to be compared then S_a calibration will be an important part of our experimental procedure.

Response to Referee #3

This is a fairly well written description of a system for studying the growth of ice crystals in the atmosphere. How crystals grow and what determines their distribution of habit and size is a very important question for meteorology, and this paper represents significant progress in answering that question. I do have some comments on the paper however. If these are adequately dealt with, this paper definitely should proceed to publication in the journal.

Our Reply: We thank the reviewer for their helpful suggestions. Here are the changes made to the revised manuscript:

Page 2 line 10; there is the statement "Neither effect typically occurs for cloud crystals". This needs some substantiation, at least in regard to the proximity of other growing crystals. Could the authors provide an estimate of the concentration of ice nuclei in a typical cloud?

Our Reply: We have clarified the text with references to typical number concentrations in ice clouds.

Section 2. This section purports to list several issues, and how they are solved in the CC2 design. The latter part of this aim seems to have been forgotten by the time point 5 is reached - there is plenty of discussion of the issues associated with capillaries interacting with crystal faces or vertices, but this is not tied to the CC2 design. This section would also be easier to follow if it were organized with subsections, rather than a list.

Our Reply: We have clarified the purpose of this section and added subsection headings in bold to increase the readability of this section.

Section 3. Snowmax is apparently a trademark? A reference to a supplier (or a recipe when the name is first used) should be provided.

Our Reply: We have added a footnote to the Snomax supplier. The recipe for the Snomax solution used is discussed in Wood et al. 2002 and we have included this reference.

Reference list; the two references to Swanson and Nelson (2019 a,b) are quite inadequate!

Our Reply: This manuscript is one of the first describing experiments done in the new CC2 instrument. Unfortunately all manuscripts describing the results from this work are not yet submitted for publication. In keeping with convention we have added "Unpublished Manuscript" to these references.

Another very minor point is in the opening sentence of the second paragraph (of section 1) the authors do seem to like the work "likely" overmuch.

Our Reply: Indeed annoying.... We have rewritten the sentence.

Low-Temperature Triple-Capillary Cryostat for Ice Crystal Growth Studies

Brian D. Swanson¹ and Jon Nelson²

¹ESS Department, University of Washington, Seattle, WA USA , Laucks Foundation Research, Salt Spring Island, BC Canada

²Redmond Physical Sciences, Redmond, WA USA; E-mail: jontne@gmail.com

Correspondence: brian@laucksfoundation.org

Abstract. Ice crystals come in a remarkable variety of shapes and sizes that affect a cloud's radiative properties. To better understand the growth of these crystals, we built an improved capillary cryostat (CC2) designed to reduce potential instrumental artifacts that may have influenced earlier measurements. In CC2, a crystal forms at the end of one, two, or three well-separated, ultra-fine capillaries to minimize both potential crystal-crystal and crystal-substrate interaction effects. The crystals can be initiated using several ice-nucleation modes. The cryostat has two vapor-source chambers on either side of the growth chamber, each allowing independent control of the growth chamber supersaturation. Crystals can be grown under a range of air pressures, and the supersaturation conditions in the growth chamber can be rapidly changed by switching between the two vapor-source chambers using a sliding valve. Crystals grow fixed to the capillary in a uniform, stagnant environment and their orientation can be manipulated to measure the growth rate of each face. The high thermal-mass of CC2 increases the stability and uniformity of the thermodynamic conditions surrounding the crystals. Here we describe the new instrument and present several sample observations.

Copyright statement. Text copyright

1 Introduction

Ice crystals are important in the radiation balance of the Earth's climate system (Liou and Yang, 2016; Heymsfield et al., 2017).

But we still lack knowledge of both the crystal-shape distribution in ice clouds and the processes responsible for the observed variation in crystal shapes. Previous studies have used a variety of techniques to grow ice crystals under simulated tropospheric conditions, but each experiment seems to give different normal growth rates (i.e., rate of face advancement normal to itself), even under similar conditions and using similar techniques. [For example at -15°C see Beckmann and Lacmann \(1982\); Lamb and Scott \(1983\)](#) and [at -30°C see Kobayashi \(1965\); Sei and Gonda \(1989a\); Gonda and Kojima \(1983\); Gonda et al. \(1994\); Libbrecht \(2003\).](#)

Why is this?

At low supersaturations, some of the variability is likely due to crystal defects, [and the defect structure likely varies from one face to another, with much of the structure likely arising from nucleation of the crystal as the ice nucleation process is expected to](#)

leave each crystal facet with a different defect structure. However, as described in Nelson and Knight (1996), the variations may also be caused by potential instrumental artifacts. For example, in growing crystals on a flat substrate (e.g., Shaw and Mason (1955); Hallett (1961); Lamb and Scott (1972); Beckmann and Lacmann (1982); Sei and Gonda (1989a)), the substrate-crystal edge could be a preferred site for new layer nucleation that does not exist without the substrate. Such substrates can also have 5 epitaxial-induced strain effects (Cho and Hallett, 1984a, b), and the temperature gradients in the crystal can greatly reduce the growth rates over those predicted assuming equal temperatures of crystal and substrate (Nelson, 1993). Growth on fibers can have smaller, yet still significant substrate effects. For example, images of small crystals grown on a thin fiber by Kobayashi (1958, 1961) show the fiber often exiting at a crystal corner or edge, which could be showing substrate-induced control over the crystal aspect ratio, but without the capability of rotating the fiber, one cannot rule out the possibility of fiber influence 10 on the other cases as well. Similar questions regarding control of habit by the fiber can be seen in the small crystals in Bailey and Hallett (2004). When the crystals grow away from the fiber, as in the larger crystals in Bailey and Hallett (2004), growth may occur on only one side of the fiber and the crystals may be close enough together to impede each other's growth rates through the vapor-density field (Westbrook et al., 2008). Neither effect typically occurs for cloud crystals as the number density, during the vapor growth phase, typically ranges from 0.1 to 10 crystals per cm³ (Mace et al., 2001; Kärcher and Strom, 2003) 15 so average crystal-crystal separation is typically mm (or more) in scale. In addition, many apparatuses have temperature and supersaturation gradients within the chamber that make calculating the precise thermodynamic conditions difficult.

Several support-free methods were developed that reduce the potential for crystal-substrate interaction effects but they can have other issues. In vertical wind tunnels and cloud chambers (i.e., Yamashita (1973, 1974); Gonda (1980); Takahashi and Fukuta (1988); Takahashi et al. (1991)), it is difficult to control the growth conditions precisely. Here Also here the crystal 20 seeding, which typically occurs near the top of the chamber, leads to crystal fall motions that makes it difficult to continuously monitor the growth of individual crystal faces throughout the experiment. Electrodynamic levitation methods avoid potential crystal-crystal interaction effects but the rapid motion of the crystals makes high-clarity imaging from a variety of crystal orientations difficult (Swanson et al., 1999; Bacon et al., 2003; Magee et al., 2006; Harrison et al., 2016) . All support-free methods have the potential disadvantage of ventilation factors that can enhance the crystal growth rates of oscillating crystals. 25 Finally, wall-ice formation is a general concern in most laboratory experiments because it can lower the supersaturation (S) in the chamber and the changes in S could go be unnoticed by an experimenter without an independent method of following S throughout the experiment.

To observe crystal growth at low temperatures while minimizing such instrumental shortcomings, we built a new instrument called capillary cryostat 2 (CC2). The design is an improvement over the capillary device in Nelson and Knight (1996), hereafter 30 CC1, in which the ice crystal grew at the tip of an ultra-fine glass capillary. Like the earlier device, CC2 practically eliminates temperature gradients, greatly reduces substrate effects, and allows all crystal faces to be monitored in a highly controlled, uniform environment. But in addition, CC2 allows experimenters to follow the growth of, and possible interactions between, several crystals growing under identical conditions. Also, CC2 It has two vapor-source chambers for observing the effects of making rapid supersaturation changes and for independent temperature and supersaturation control, as well as for allowing

~~control of~~ and has an associated vacuum system and gauges for control of the growth chamber air pressure. To date, ~~it~~ CC2 has proven useful for studying the formation and behavior of air pockets in ice (Nelson and Swanson, 2019).

2 New CC2 Instrument and Methods

The design is basically a 'box within a box within a box' (see Figs. 1 and 2). At the center is the 13 cm x 7.5 cm x 20 cm experimental chamber EC with its 3 chambers - the growth chamber is near the middle with vapor-source chambers both above and below. Figure 2 shows the growth chamber GC containing the growing or sublimating crystals of interest. The crystals sit on the ends or sides of three well-separated, pure-silica glass capillaries that extend down about 3-cm from the ceiling of the GC. Individual or multiple ice crystals can be suspended on each capillary. The upper and lower vapor-source chambers VSC control the humidity within the GC. A sliding valve blocks one or the other VSC from the GC. An actuator mechanism attached to the sliding valve allows the experimenter to select which VSC is actively setting the GC humidity. Inside each VSC is a vapor source VS mounted on top of a thermoelectric cooler TEC module. Each VS is typically filled with frozen high-purity liquid-chromatography HPLC water. The supersaturation or sub-saturation conditions inside the VSC are controlled by the temperature (T_{VS}) of the VS. Surrounding the EC is an optically clear liquid-cryogenic fluid (typically methanol or a silicone fluid) contained within the bath box. The bath box itself is surrounded by the vacuum-shroud box. A turbo-molecular pump typically evacuates the vacuum-shroud box to less than 10^{-5} torr to isolate and insulate the EC from the laboratory environment. The EC, bath box, and vacuum-shroud box have silica windows front and back for illumination and imaging of the ice crystals. The imaging is done (at a working distance of about 80 mm) ~~using a combination of back and with a choice of back or~~ front illumination and Nikon SLR cameras attached to Leica tele-microscopic zoom lenses. The EC and VS temperatures and pressure are monitored using a LabView data acquisition program, HP switch/multiplexer, and a 5 1/2 digit digital multi-meter.

2.1 Instrumental issues addressed by CC2 design

We now describe how the CC2 design addresses several potential instrumental issues ~~that may have influenced results from previous methods, and how the capillary method can be used to obtain reliable data sets.~~

1) Temperature stability and gradients in the instrumental chamber

Small changes in crystal temperature can have large effects on ice crystal shape. Near liquid-water saturation, a few $^{\circ}\text{C}$ change near -8°C changes long columns into thin tabular crystal forms (Takahashi et al., 1991). At low supersaturations, small temperature changes may significantly effect facet-normal growth rates since this rate can depend exponentially on ~~the vapor source temperature~~ T_{VS} (via its control of supersaturation) when the face is free of new-layer-generating defects (i.e., "perfect" faces, which were commonly found in CC1).

The stability of two temperatures, that of the experimental chamber T_{EC} and that of the ambient air surrounding the crystal T_a , are important ~~to discuss~~. The temperature stability of the EC is set by 1) the cryogenic refrigerant temperature control from a Neslab ULT-80 bath-circulator unit (temperature stability exceeds 0.1°C over a 3-hour period), 2) the room temperature stability, and 3) the large thermal mass of the EC (which smooths short-term temperature fluctuations via its roughly 15-min response time). Specifically, the EC was milled from a single block of tellurium-copper, then nickel plated on the outside and gold plated inside for surface uniformity and to reduce the potential for oxide formation and contamination. Temperature variations in T_a will be due to temperature fluctuations and gradients in the internal walls of the GC. A time-series measurement of the 12 thermistors buried in the walls of the EC show that the maximum fluctuation of the EC block is less than 50 mK over a 1-day period. We worried that the TECs might induce small gradients in the EC temperature but find no measurable additional thermal gradient in the GC when the TEC current $I_{TEC} < 0.5\text{A}$ - a value much larger than is needed for growth or sublimation conditions in a cold cloud. For a typical 11-hour period, the maximum gradient across the EC block was less than 10 mK. So we are comfortable assuming that $T_{EC} = T_a$ to within a few mK.

~~2) Precise control and stability of supersaturation around the crystal. Supersaturation drives crystal growth, and therefore it must be determined precisely and reproducibly. The ambient supersaturation around the crystals in the GC~~

15 2.1.2 Precise control and stability of supersaturation around the crystal

While chamber temperature is relatively straightforward to measure and control, precise supersaturation measurement within a chamber along with measurement and control near the surface of a growing crystal is much more difficult. In any experiment we are concerned with both spatial and temporal gradients in the growth chamber supersaturation S_{GC} . The "gold standard" for crystal growth experiments involves two parts: a stable, controlled and gradient-free S_{GC} within the experimental chamber, and the measurement of S_a is set by S_{VS} (the supersaturation at the surface of the VS), and may differ from S_{VS} due to nearby crystals or wall ice in the EC. For growth-sublimation-growth experiments, one vapor source is set to give the desired growth condition and the other is set to the desired sublimation condition. Each VS consists of a gold-plated copper disc, machined such that the top portion forms a cup shape that holds up to surface of the growing (or sublimating) crystal at the same time the crystals are growing (or sublimating). No ice crystal growth rate experiment to date satisfies these 2 g of water. Each VS has an exposed surface area of about 6 cm^2 . As the typical grown crystal is less than 0.05-cm across, the VS surface area is usually more than 1000 times larger than the crystal being studied, and, in the absence of other crystals or wall ice, conditions. But the method used in CC2, although not yet at the "gold standard" level, has enhanced thermal stability and a relative gradient-free nature that is a large improvement over previous methods.

Within CC2 all crystals grow simultaneously within an approximately 1 cc volume near the center of the GC. Simultaneous growth in a chamber without gradients means all crystals experience the same thermodynamic conditions. Sequential growth experiments cannot claim all crystals experienced "the same" thermodynamic conditions without an actual measurement of $S_a = S_{VS}$. This supersaturation is determined by the vapor-source temperature, which is controlled by setting I_{TEC} . The design improves upon that used in CC1 (Nelson and Knight, 1996) which used the solute method alone, although solutes can be used in the VSC as well. Knowing the ambient temperature of the air (or wall temperature) in the growth chamber T_a ,

the vapor-source temperature T_{VS} , and noting that the area of the VS ice surface greatly exceeds that of any other ice in the system, then the ambient supersaturation in % equals. Previous experiments have assumed gradient-free conditions and in this case the ambient supersaturation at the crystal surface given in % by

$$S_a = \frac{N_{eq}(T_{VS}) - N_{eq}(T_a)}{N_{eq}(T_a)} * 100, \quad (1)$$

5 where N_{eq} is the equilibrium vapor density in #molecules/m³. To estimate the precision of and T_a is the temperature at the crystal surface. It is possible that other factors affect S_a so in future experiments we will test the use of this equation. Other than the effect of thermal gradients within the EC (which are minimal as discussed above), the experiment, note that the potential gradients in S_{GC} within the GC can come from 3 potential sources: a) thermal instability of T_{VS} , b) gradients within the VS itself, and c) the presence of other ice crystals within the EC.

10 a) **Thermal stability of T_{VS} .** The numerator in eq. (1) is to first order proportional to the ice surface-temperature elevation $\Delta T = T_{VS} - T_a$. Thus, the relative uncertainty in supersaturation $\delta S_a / S_a = \delta \Delta T / \Delta T$. With feedback TEC temperature control the VS temperature standard deviation ΔT is typically about 3 mK (the variation observed over several hours). This gives an estimated uncertainty in S_a of about 0.03%. To understand the meaning of 0.03% supersaturation, consider that an ice crystal growing at the maximum possible rate at -30°C at this supersaturation is about 60 μm per hour in a pure vapor (from 15 the Hertz-Knudsen equation (e.g., eq. 1 of Holyst et al. (2015). This equation assumes a rough surface, or $\alpha = 1$), then we expect the uncertainty to add about 0.2 μm per hour additional growth to a 100- μm diameter spherical crystal in an atmosphere of air (Maxwell's expression or Hertz-Knudsen divided by the vapor-diffusion impedance). This uncertainty is less than the measurement resolution over several hours growth. When other crystals are nearby, then S_a describes an intermediate value. For the growth of 3 ice crystals each less than 500 μm in size and separated by least 5 mm then we can assume $S_a = S_{VS}$ to 20 within 10% of

b) **Thermal gradients within the VS.** Each VS consists of a gold-plated copper disc, machined such that the top portion forms a cup-shape that holds up to 2 g of water. Each VS has an exposed surface area of about 6 cm². As the typical grown crystal is less than 0.05-cm across, the VS surface area is usually more than 1000 times larger than the crystal being studied, and, in the absence of other crystals or wall ice, $S_a = S_{VS}$. This supersaturation is determined by the vapor-source temperature, 25 which is controlled by setting I_{TEC} . The design improves upon that used in CC1 (Nelson and Knight, 1996) which used the solute method alone, although solutes can be used in the VSC as well.

Consider now the temperature difference between the thermistors imbedded in the VS cup T_{VS} and the surface of the VS ice T_{VSS} . In general, we need this difference to be much less than the set temperature rise of the VS cup over that of the environment ΔT ; otherwise, our inferred supersaturation will be too high. To estimate $\frac{T_{VS} - T_{VSS}}{\Delta T}$, assume a steady state in 30 which the rate of latent-heat loss at the source-ice surface (during a crystal-growth experiment) equals the sum of the i) rate of heat conduction through the VS ice plus ii) the heat loss from the surface to the surroundings. Consider just i) first. Assuming that the number of molecules of water leaving the VS ice per second equals the number depositing on the observed crystal on a capillary (i.e., steady-state), and using the Clausius-Clapeyron equation, this ratio can be shown to equal $\frac{R}{S_a} L A_r \left(\frac{k_B \beta^2}{\Omega \lambda} \right)$, where R is the surface-averaged normal growth rate of the crystal (i.e., normal to the surface), L is the average thickness of the

VS ice, A_r is the ratio of areas between the observed crystal and the VS ice, k_B is Boltzmann's constant, β is the latent heat per molecule normalized by $k_B T$, Ω is the volume per molecule in solid ice, and λ is the thermal conductivity of ice. This last factor in parenthesis involves only material properties and equals about 1×10^8 s/m². Using $R = 5 \mu\text{m}$ per hour, $S_a = 0.01$ (1%), $L = 1 \text{ cm}$, and $A_r = 10^{-3}$, this ratio is 10^{-4} . As these are roughly maximum values, we can generally assume the temperature offset to be negligible. (Also, as the factor depends on L/λ , the influence of temperature gradients in the vapor-source cup itself should be negligible due to the tellurium copper having a thermal conductivity nearly 200 times larger than that of ice (and L being smaller).) ~~However, if frost forms elsewhere on the walls, this ratio may become significant due to a large increase in A_r . This consideration is considered in more detail in 3) below.~~

Concerning ii), the heat loss to the surroundings, there are four to consider: conductive loss from the ice to the air, conductive loss from the VS cup to the cup holder, convective loss to the air, and radiative loss to the walls. For the conductive loss to the air, we can estimate the effect by equating the heat flow through the ice to the heat flow through the air via ~~convection~~conduction. The resulting temperature shift in the ice divided by $(T_{VSS} - T_a)$ (i.e., ΔT less the temperature shift in the ice) will equal the ratio of the conduction distances times the inverse ratio of the thermal conductivities. The first factor is about 1/3, and the second is about 0.015/2.1. Thus, this temperature shift is only about 1/300 of that of ΔT and can be ignored. The conductive loss from the VS cup to the cup holder would create gradients in the cup holder. However, the thermal conductivity of the Te-Cu cup is about 4000x that of the rubber o-ring holding it in place and nearly 40,000x that of the air gap. Thus, even though this gap is small, we can neglect the resulting thermal gradients in the cup. ~~For the convective heat loss from the ice surface, this can only occur when we heat the ice~~

~~The heat loss can also be convective if the vapor source is heated~~ for growth experiments, and requires a critical temperature difference between the ice surface and the top wall of the VSC. (If we instead use solute, as was done in CC1, then the issue cannot arise.) For growth experiments, the resulting convection may significantly cool the ice surface, so our aim is to stay below the critical temperature. If we assume that the onset of convection occurs with a Rayleigh number of about 1500, ~~then we must keep (following Saxena et al. (2018), where this number is proportional to the cube of the chamber height, the temperature difference between wall and source, and properties of the air), then for our chamber and operating temperature, staying below this Rayleigh number requires~~ the ice surface ~~lie~~ within about 0.5 K of the wall temperature. Finally, the influence of the radiative heat flux is considered in 4.2.1.4) below.

c) ~~The presence of other crystals. We consider two cases separately: a few crystals very near the monitored crystal of interest and a large number of crystals on the wall as frost. The later case is discussed in 2.1.3 below; here we focus on the former. When other crystals are nearby a crystal of interest then S_a can be less than S_{VS} even when the area of the VS ice surface greatly exceeds that of any other ice in the system.~~ In the case of the simultaneous growth of several observed crystals, the supersaturation near an observed crystal may be reduced due to the proximity to other crystals. Westbrook et al. (2008) estimate a 3-fold reduction in growth rate for close crystals along a fiber, a situation that simulated those in Bailey and Hallett (2004). At larger crystal separations, the effect has not been determined, but the $1/r$ dependence of the vapor-diffusion field away from a crystal suggests that to ensure a crystal-proximity effect of less than 10%, the crystals should be separated by nearly 10x their mean dimension. ~~We find (result reported elsewhere (Swanson, 2019)) about a 30% reduction in facet-normal~~

growth rate (caused by the vapor uptake by the neighboring polycrystal crystallites) for a prismatic crystal growing on top of a polycrystal as compared with similar prismatic crystals growing and separated by 100's of μm .

In CC2, the three capillaries are on non-parallel axes, and thus their separations are adjustable, allowing measurement of the proximity effect. They are easily set to be several centimeters apart, which is more than 100x their typical dimension of about 5 $100 \mu\text{m}$.

~~In other experiments (Swanson and Nelson, 2019), we have in addition used droplet evaporation measurements done simultaneously with crystal growth measurements to give a direct, and independent, estimate of S_a . In these experiments we use one capillary to hold the evaporating droplet while at the same time growing or sublimating the crystals of interest held on the other capillaries in the chamber. Results from these experiments demonstrate that, even in a carefully controlled environment, the calculated values of S_a can be different from actual measured values. We conclude that accurately predicting and maintaining a constant S_a at a chamber center without a direct measurement of the supersaturation requires careful calibration. For the growth of 3 ice crystals each less than $500 \mu\text{m}$ in size and separated by least 5 mm then we can assume $S_a = S_{VS}$ to within 10% of S_{VS} .~~

3) Frost formation on the experimental chamber walls. Frost

2.1.3 Frost formation on the experimental chamber walls

15 Frost can form on chamber walls and, if the area is large, can uptake a significant fraction of the source vapor. ~~In a~~ A highly controlled vapor-source supersaturation, S_{VS} , does not necessarily set the ambient supersaturation, S_a , at the center of the chamber where the crystals are growing if there is ~~unobserved~~ frost or condensate growing on the wall. Such ~~unobserved~~ frost is a particular problem when growing crystals sequentially because any measured difference in their rate or habit may not be inherent, but instead be due to their being affected more or less by frost. To reduce this issue, the CC2 windows allow 20 observation of all surfaces inside the GC and VSC. But it is possible that this ice is so thin as to make it nearly invisible to the eye. An important factor is the relative surface area of the frost versus that of the VS ice. If their areas and thicknesses are the same, then the vapor-density in the EC would be mid-way between the equilibrium values for the VS ice and the chamber walls. However, the effect in practice would likely be worse because the frost layers would likely be much thinner than the VS ice, pushing the vapor-density closer to the equilibrium value for the walls due to the temperature-gradient effect in 23.1.2) 25 above. ~~Thus, frost is a major concern.~~

The windows on the sides of the VSC ~~provides~~ provide for easy detection of large frost crystals and, once noticed, that chamber can be immediately sealed off. In practice, we find that when frost crystals first appear, they are in the VSC, relatively close to the source ice. For the experiments described here, the VSC and GC internal walls were continuously monitored for frost. If frost began to form in the attached VSC, then the sliding valve was changed to disconnect the VSC from the GC and 30 the TEC in the other VSC was set to maintain the desired humidity in the GC. The ability to isolate one VSC from the GC when frost first occurs and to switch to a frost-free VSC allows us to continue to grow the crystals for long periods at near-constant S_a conditions. To clear the frost off the walls of a VSC, we first evacuate the VSC and set its T_{VS} to at least 10°C below T_a . The frost typically left the walls within about 30 minutes under these conditions. For the conditions of the experiments

described here, typically no frost was observed on VSC walls for at least 6 hours. The data set here was collected before frost started to form in the GC walls.

4) ~~Radiative heating effects. This effect~~ In a future paper, Swanson and Nelson (2019), we report results from droplet evaporation measurements done simultaneous with the crystal growth measurements. Measuring the evaporation rate of pure water droplets during crystal growth does give a direct and independent measure of S_a near the growing crystals surface. For these experiments one capillary is used to hold the evaporating droplet while the other two hold the growing or sublimating crystals. Results from these experiments demonstrate that accurately predicting S_a at a chamber center requires careful calibration. For the results reported here we are concerned with facet-normal growth rate differences for crystals growing simultaneously under the same thermodynamic conditions. In these experiments the ice crystal surface area is small compared with that of the VS and no wall ice was present. We continuously measure T_{GC} and T_{VS} and the enhanced thermal stability and control within CC2 gives us confidence that, within the variations caused by the measured temperature gradient across the EC, S_a is to good approximation S_{VS} within that 1 cc volume that contains the capillary tips. In future experiments, where a detailed comparison with crystal growth models is the goal, S_a calibration measurements will be made along with the growth rate measurements.

15 2.1.4 ~~Radiative heating effects~~

~~Radiative heating~~ can occur in two places. First, consider thermal radiation between the VS surface and the VSC wall. The VS-GC temperature difference is typically less than 3.5°C - the value needed to achieve liquid-water saturation at -40°C . Due to the relatively small temperature differences involved, and also the very low emissivity of the gold plating of all interior walls, such a radiative heat transfer has a negligible influence on the VS surface temperature. Second, consider thermal radiation between the ice crystals and sources outside the windows. The ice crystals sit at T_a , but the thermal link is weak due to the crystal being surrounded by air. Considering the different materials viewed by the crystal (windows, walls, and circulating fluid), determining the influence of radiative heating on ice-crystal temperature is best handled as an experimental issue. We examine this issue by monitoring the crystals in the growth chamber under controlled conditions in which the windows are alternately exposed or covered with low IR-emissive material. When we have tried this test, we observed no IR heating effects on the normal growth rates.

25 5) ~~The effect of the capillary on crystal growth. The capillary~~

2.1.5 ~~The effect of the capillary on crystal growth~~

~~The capillary~~ holds the crystal steady, allowing clear imaging and viewing from several angles. Also, as the crystal starts at the capillary tip (typical case), one can usually measure the advance of all parts of the crystal with respect to the fixed capillary tip. Although these features are advantages of the method, the capillary can promote growth on one, two, or three faces.

Consider the examples in Fig. 3. The images show two crystals nucleated and grown at the same time, but on different capillaries, the left images from the front capillary Cf, the right images from the back capillary Cb. The crystal on the left (a, b) is nearly a hexagonal prism, but by measuring the distance from the capillary tip along the surface normal, one finds

that the top right prism face has grown about 25% faster than the others. The capillary is seen exiting the crystal at the vertex between this face and the top left prism. Subsequent images (not shown here) show the crystal growing larger, but the capillary remaining at this vertex. As the vertex stays at the capillary, these observations show that the capillary determines the relative normal growth rates of these two faces. The rotated view in (b) shows that the two basal faces have nearly equal normal growth rate, and neither is contacted by the capillary. Thus, the basal faces appear unaffected by the capillary. So, of the eight crystal faces, two are directly compromised by the capillary, but six are not directly influenced. In using data from this crystal, we must consider the influence that the faster growth on the top two prism faces have on the vapor diffusion field near the other faces and the crystal temperature. In this way, the influence of the capillary may be overcome by crystal-growth modeling. The exact method will be described in a later publication.

10 The crystal on the back capillary, c-f in Fig. 3, shows further limitations and features. In this case, we cannot see the location of the capillary inside the crystal and must instead estimate its location by examining the growth sequence starting from nucleation (not shown). Nevertheless, the basal-side views in (c) and (f) show that the capillary does not contact the basal faces (except possibly from the ice interior), yet one basal face grew faster than the other. Moreover, views (d) and (e), show that this crystal has two opposite prism faces that are much larger in area, and thus have much lower growth rates. The overall shape is
15 similar to that proposed for crystals that generate the Parry arc (Westbrook, 2011).

Finally, consider the crystal in Fig. 4. In this case, the capillary exits at a corner, thus contacting one basal and two prisms. As in other cases like this observed during both CC2 and CC1 experiments, the crystal does not start this way, but once the corner reaches the capillary, it always remains there (at least under constant conditions). Why does this occur? Clearly, the introduction of an interior glass-ice corner should promote new layer nucleation. If such a site is the most active on a given
20 face, then that site will increase the normal growth rate of the face. Moreover, if this capillary is tilted towards a neighboring face, then the relative increase in growth rate over that neighboring face will bring the edge between the two faces closer to the capillary. Once the edge reaches the capillary, it will stay there because the same promotion of layer nucleation will occur on the neighboring face. In three dimensions, if the capillary also tilts towards a third face, this process will bring that face to the capillary until the capillary exits at the common corner. However, if the layer-nucleation-promotion effect is relatively
25 weak, then supersaturation gradients or a surface defect site may produce more rapid layer nucleation elsewhere, such as at a nearby crystal corner. Thus, there are cases where, despite such promotion of layer nucleation, the face growth is controlled by a more active site, making the capillary influence irrelevant. For example, if the capillary exits the crystal from near the face middle, it will likely lie at a lower-supersaturation region, with the more active step-generation site instead being at the corner. In such a case, the capillary may have a small local influence, but not influence the normal growth rates of the faces.
30 These considerations also apply to crystals grown not at the tip, but midway along a capillary or any fiber. This explains why, for example, that in previous high-supersaturation experiments, the rapid-growing parts of the crystal are away from the fiber (e.g., Nakaya (1954); Kobayashi (1958); Bailey and Hallett (2012)).

Occasionally, we observe indications of different influences from the capillary. For example, the crystal can appear to avoid contact with the capillary. This appears to be a vapor-shielding effect because it only occurs when the crystal size is within
35 a few diameters of the capillary tip and only occurs where the crystal contacts the capillary. Other parts of the crystal are

unaffected, and the effect vanishes when the crystal grows larger. Another effect that can occur is rapid growth up the capillary in which the growth appears as smaller crystals of the same orientation. It is possible that this crystallization may be a result of thin-film crystallization on the glass capillary after a crystal nucleates at the tip. Both of these influences should be smaller with smaller-diameter capillaries, and may also be reduced with suitable coatings. Finally, within the ice just adjacent to the 5 capillary (within a few capillary diameters), the interface may create strain effects in the ice. To date, we have not seen evidence of such effects, but they remain a possibility.

Thus, the capillary influence on new-layer production can be irrelevant in some cases and may be overcome using modeling in other cases, but should always be examined. Acknowledging this influence has two additional benefits. One, we may use it to study the nucleation process itself. Two, we can recognize the effect in other studies and realize that the resulting data may 10 not be reliable. In future experiments, we plan to research these effects and develop strategies for quantifying their influence.

3 Growth of Snomax-Nucleated Crystals

Finally, we describe a case in which we nucleated crystals using Snomax ice nuclei-a Snomax-water solution¹ and grew them for several days at low temperature and low supersaturation. Before insertion of the crystals the GC was prepared as follows: a) The internal GC walls were washed with acetone, ethanol, and finally with HPLC water. b) After window cleaning and 15 re-assembly, the GC was flushed for over an hour with dry nitrogen and then the cooling began with the ULT-80 set to 0°C. c) The VS cups were loaded with HPLC water and each TEC was set such that T_{VS} remained about -10°C below T_a , d) A slow cool-down was then initiated to the experimental temperature. Keeping the VS frozen with the above procedure avoided fogging of the GC windows and reduced the possibility of ice forming on the inside walls of the EC. Once the desired T_a was established then T_{VS} was set to produce the desired supersaturation S_{VS} and the capillaries were inserted into CC2. Unlike 20 the nucleation method used for the previous crystals, this one produced several crystals along each capillary. We report just on the ones at the ends of capillary Cf and Cr.

All crystals began the experiment as near-identical $\sim 20 \mu\text{m}$ diameter liquid droplets of a Snomax-HPLC water solution. The 5 μm diameter capillaries were dipped into a Snomax solution made similar to Wood et al. (2002) and then inserted into CC2. The experiment was broken into two phases – Part A (which lasted 45 hours; $t = -45$ hrs to $t = 0$) directly followed 25 by part B (which lasted 47 hours; $t = 0$ to $t = 47$ hrs). For the entire 92 hours the growth chamber temperature T_a was held at -29.8°C . During part A, the crystals grew from the 20 μm frozen droplets into a variety of crystal shapes. During part A S_a was not highly controlled but conditions were maintained such that $-0.5\% < S_a < 0.5\%$ the crystals grew for 28.5 hrs with $S_{VS} \sim 5\%$; followed by 9.5 hrs of no-growth with $-0.5 < S_{VS} < 0.5\%$ (after which some facet edge-rounding was observed); followed by an 7 hour growth period with $S_{VS} \sim 2\%$. During part B S_a was controlled S_{VS} was maintained such 30 that $T_{VS} = -29.3 \pm 0.4^{\circ}\text{C}$ resulting in $S_{VS} = 5\%$.

Figure 5 shows the crystals at both $t = 0$ and $t = 47$ hrs. The images have been magnified and crystal sizes are shown in Fig. 6. We define $a(t)$ as the growth normal to the prism face and $c(t)$ as the growth normal to the basal face. The value of a and c

¹Snomax is a common ice nucleant used for making artificial snow at ski resorts, and is a product of York International, Victor, New York, 14564.

are diameters in these two normal directions. (Thus, they include measurements normal to faces potentially influenced by the capillary as discussed above.) The aspect ratio $AR = c/a$. In the lower image of crystal Cf, we see that the upper basal face, which is contacted by the capillary, grew faster than the lower facet. But for crystal Cr, the lower image shows the two basal faces to have nearly the same normal growth rate, and neither is contacted by the capillary. Thus, for the basal faces, Cf has 5 one that is likely possibly affected by the capillary, but Cr appears unaffected by the capillary.

Since at least Gonda and Koike (1983), we have known that prismatic crystal aspect ratios can be different for similar growth conditions. The case here is consistent with this finding. In particular, we also find that the crystals in Fig. 5 responded to T_a and S_a in different ways. Comparing crystal shape at the beginning and end (AR_0) and end (AR_{47}) of part B, we find for Cf, $AR_{47}/AR_0 = 0.62$, while for Cr, $AR_{47}/AR_0 = 1.61$. This illustrates that, under the same conditions, a crystal can grow more 10 plate-like at the same time another crystal is growing more column-like. (Concerning the capillary influence - the potential promotion of growth on one basal for Cf and one or two prisms for Cr oppose this trend. Thus, it is likely this finding is not due to a capillary influence.) The relative growth rates shown in Fig. 6 for the two crystals are also quite different. Both crystals ended part A of the experiment with tabular habits. But the thinner plate (Cr with $AR = 0.46$ $AR_0 = 0.46$) grew during part B to be more columnar, while the thicker plate (Cf with $AR = 0.72$ $AR_0 = 0.72$) grew to be more tabular. This behavior is also 15 clear from the relative growth rates (indicated generally by the slope of the curves) in the \hat{a} and \hat{c} directions. The curves in Fig. 6 are from a simple two-parameter fit to the data set. We see here that a simple $t^{1/2}$ parameterization (where t is the time) for both $c(t)$ and $a(t)$ fits well. With or without capillary influence the growth of both crystals is well described by a similar parabolic growth model as has been found for spherical droplets (Fukuta and Walter, 1970). A more detail discussion of these results is reported elsewhere (Swanson, 2019).

20 Crystals in previous experiments were often grown sequentially, making it difficult to ensure the exact same conditions were reproduced. Moreover, in many cases, experimenters were unable to follow the development of each crystal, and each crystal face, throughout the growth process. In our experiments, several well-separated crystals can be grown simultaneously and experience the same thermodynamic conditions. The crystals remain prismatic during the multi-day growth period, but 25 large variations in AR and growth rate in the \hat{a} and \hat{c} directions are observed. Such variations in AR turn out to be typical for prismatic crystals (Bacon et al., 2003; Swanson, 2019) and show control of growth shape is likely via defect-driven surface processes. By using CC2 to measure the growth of individual crystal faces for a wide range of conditions we will be able to quantify the variability of facet normal growth rates.

4 Conclusions

We have built a new instrument to measure high-precision growth rates of ice crystals and droplets at temperatures down 30 to -60°C . Preliminary observations have shown the advantage of following individual faces of multiple crystals in the CC2 apparatus. With CC2, thermodynamic control is much tighter than has been reported for previous instruments. The ability to grow multiple crystals under identical thermodynamic conditions, starting from their nucleation and following each face over long time periods, as well as being able to track and remove frost during the experiment, gives us confidence that differences

in observed behavior can be distinguished from instrumental effects. We expect the method will be complementary to our substrate-free electrodynamic balance methods (Bacon et al., 2003). To check these results, future experiments that combine both techniques are planned.

Author contributions. BS and JN designed and assembled the new instrument. BS and JN designed the experiments and carried them out.

- 5 BS developed the Labview data acquisition code, made the figures and prepared the manuscript with contributions from JN.

Competing interests. The authors declare that they have no conflict of interest.

Acknowledgements. We thank Chris Foreman at Foreman CNC Machining LTD, Dave [Shatford](#) at Met-All-Fab in Sidney BC and Glenn

Ryan at Limited Productions Inc. Bellevue WA for assistance with the fabrication of the instrument. We thank Hawk Ridge Systems for

providing a copy of SolidWorks CAD software. We thank Mary Laucks for helpful comments on this manuscript. This work is supported by

- 10 the National Science Foundation grant AGS-1348238 and by the Laucks Foundation.

References

Bacon, N. J., Baker, M. B., and Swanson, B. D.: Initial stages in the morphological evolution of vapor grown ice crystals: A laboratory investigation, *Quart. J. R. Met. Soc.*, 129, 1903–1927, 2003.

Bailey, M. and Hallett, J.: Growth rates and habits of ice crystals between -20 and -70 C, *J. Atmos. Sci.*, 61, 514–544, 2004.

Bailey, M. and Hallett, J.: Ice Crystal Linear Growth Rates from -20 to -70C: Confirmation from Wave Cloud Studies, *J. Atmos. Sci.*, 69, 390–402, 2012.

Beckmann, W. and Lacmann, R.: Interface kinetics of the growth and evaporation of ice single crystals from the vapour phase II. Measurement in a pure water vapor environment, *J. Cryst. Gr.*, 58, 433–442, 1982.

Cho, N. and Hallett, J.: Epitaxial ice crystal growth on covellite (CuS) I. Influence of misfit strain on the growth of non- thickening crystals, *J. Cryst. Gr.*, 69, 317–324, 1984a.

Cho, N. and Hallett, J.: Epitaxial ice crystal growth on covellite (CuS) II. Growth characteristics of basal plane steps, *J. Cryst. Gr.*, 69, 325–334, 1984b.

Fukuta, N. and Walter, L. A.: Kinetics of Hydrometeor Growth from a Vapor-Spherical Model, *J. Atmos. Sci.*, 27, 1160–1172, 1970.

Gonda, T.: The influence of the diffusion of vapor and heat on the morphology of ice crystals grown from the vapor, *J. Cryst. Gr.*, 49, 173–181, 1980.

Gonda, T. and Koike, T.: Growth mechanism of single ice crystals growing at a low temperature and their morphological stability, *J. Cryst. Gr.*, 65, 36–42, 1983.

Gonda, T., Matsuura, Y., and Sei, T.: In situ observation of vapor-grown ice crystals by laser two-beam interferometry, *J. Cryst. Gr.*, 142, 171–176, 1994.

Hallett, J.: The growth of ice crystals on freshly cleaved covellite surfaces, *Philos. Mag.*, 6, 1073–1087, 1961.

Harrison, A., Moyle, A. M., and Hanson, M.: Levitation Diffusion Chamber Measurements of the Mass Growth of Small Ice Crystals from Vapor, *J. Atmos. Sci.*, 73, 2743–2758, 2016.

Heymsfield, A. J., Krämer, M., Luebke, A., Brown, P., Cziczo, D. J., Franklin, C., Lawson, P., Lohmann, U., McFarquhar, G., Ulanowski, Z., Kramer, R., Luebke, A., Brown, P., Cziczo, D. J., Franklin, C., Lawson, P., Lohmann, U., Mcfarquhar, G., Ulanowski, Z., and Tricht, K. V.: Cirrus Clouds, in: *Ice Formation and Evolution in Clouds and Precipitation: Measurement and Modeling Challenges* Ice Formation and Evolution in Clouds and Precipitation: Measurement and Modeling Challenges, edited by McFarquhar, G., vol. 58, American Meteorological Society, 2017.

Holyst, R., Litniewski, M., and Jakubczyk, D.: A molecular dynamics test of the Hertz–Knudsen equation for evaporating liquids, *Soft Matter*, 11, 7201–7206, 2015.

Kärcher, B. and Strom, J.: The roles of dynamical variability and aerosols in cirrus cloud formation, *Atmos. Chem. Phys.*, 3, 823–838, 2003.

Kobayashi, T.: On the Habit of Snow Crystals Artificially Produced at Low Pressures., *J. Met. Soc. Japan*, 36, 193–208, 1958.

Kobayashi, T.: The growth of snow crystals at low supersaturation, *Phil. Mag.*, 6, 1363–1370, 1961.

Kobayashi, T.: Vapour growth of ice crystal between -40 and -90 C, *J. Meteorol. Soc. Jpn.*, 43, 359–367, 1965.

Lamb, D. and Scott, W. D.: Linear Growth rates of ice crystals grown from the vapor phase, *J. Cryst. Gr.*, 12, 21–31, 1972.

Libbrecht, K. G.: Growth rates of the principal facets of ice between -10 and -40 C, *J. Crystal Gr.*, 247, 530–540, 2003.

Liou, K.-N. and Yang, P.: *Light Scattering by Ice Crystals*, Cambridge University Press, 2016.

Mace, G. G., Clothiaux, E. E., and Ackerman, T. P.: The Composite Characteristics of Cirrus Clouds: Bulk Properties Revealed by One Year of Continuous Cloud Radar Data The Composite Characteristics of Cirrus Clouds: Bulk Properties Revealed by One Year of Continuous Cloud Radar Data, *J. of Climate*, 14, 2185–2203, 2001.

Magee, N., Moyle, A. M., and Lamb, D.: Experimental determination of the deposition coefficient of small cirrus-like ice crystals near -50 C, *Geophys. Res. Lett.*, 33, L17813, doi:10.1029/2006GL026665, 2006.

Nakaya, U.: *Snow Crystals, Natural and Artificial*, Harvard University Press, 1954.

Nelson, J.: Heat conduction problems in crystal growth from the vapor, *J. Cryst. Gr.*, 132, 538–550, 1993.

Nelson, J. and Knight, C.: A new technique for growing crystals from the vapor, *J. Cryst. Gr.*, 169, 795–797, 1996.

Nelson, J. and Swanson, B. D.: Lateral facet growth of ice and snow I: observations and applications to secondary habits, *Submitted to Atmos. Chem. Phys.*, 2019.

Saxena, A., Kishor, V., Singh, S., and Srivastava, A.: Experimental and numerical study on the onset of natural convection in a cavity open at the top, *Physics of Fluids*, 30, 057102, 2018.

Sei, T. and Gonda, T.: Growth rate of polyhedral ice crystals growing from the vapor phase and their habit change, *J. Meteorol. Soc. Jpn.*, 67, 495–502, 1989a.

Sei, T. and Gonda, T.: The growth mechanism and the habit change of ice crystals growing from the vapor phase, *J. Cryst. Gr.*, 94, 697–707, 1989b.

Shaw, D. and Mason, B.: The growth of ice crystals from the vapour, *Philos. Mag.*, 46, 249–262, 1955.

Swanson, B.: The influence of facet-normal growth rates on ice crystal shape evolution at -30C, *Unpublished Manuscript*, 2019.

Swanson, B. and Nelson, J.: On the use of droplet evaporation to measure supersaturation at low-temperature, *Unpublished Manuscript*, 2019.

Swanson, B., Bacon, N., Davis, E., and Baker, M.: Electrodynamic trapping and manipulation of ice crystals, *Quart. J. R. Met. Soc.*, 125, 1039–1058, 1999.

Takahashi, T. and Fukuta, N.: Supercooled cloud studies on the growth of snow crystals between -4 and -20C, *J. Meteor. Soc. Japan*, 66, 841–855, 1988.

Takahashi, T., Endoh, T., Wakahama, G., and Fukuta, N.: Vapor diffusional growth of free-falling snow crystals between -73 and -23 C, *J. Meteorol. Soc. Jpn.*, 69, 15–30, 1991.

Westbrook, C.: Origin of the Parry arc., *Q.J. R. Meteorol. Soc.*, 137, 538–543, 2011.

Westbrook, C., Hogan, R., and Illingworth, A.: The capacitance of pristine ice crystals and aggregate snowflakes, *J. Atmos. Sci.*, 65, 206–219, 2008.

Wood, S., Baker, M., and Swanson, B.: New instrument for studies of homogeneous and heterogeneous ice nucleation in free-falling super-cooled water droplets, *Rev. Sci. Inst.*, 73, 3988–3996, 2002.

Yamashita, A.: On the trigonal growth of ice crystals, *J. Meteorol. Soc. Jpn.*, 51, 307–317, 1973.

Yamashita, A.: Ice crystals grown in free fall in a large cloud chamber, *Meteor. Res. notes of the Japan Meteor. Soc.*, 123, 813–860, 1974.

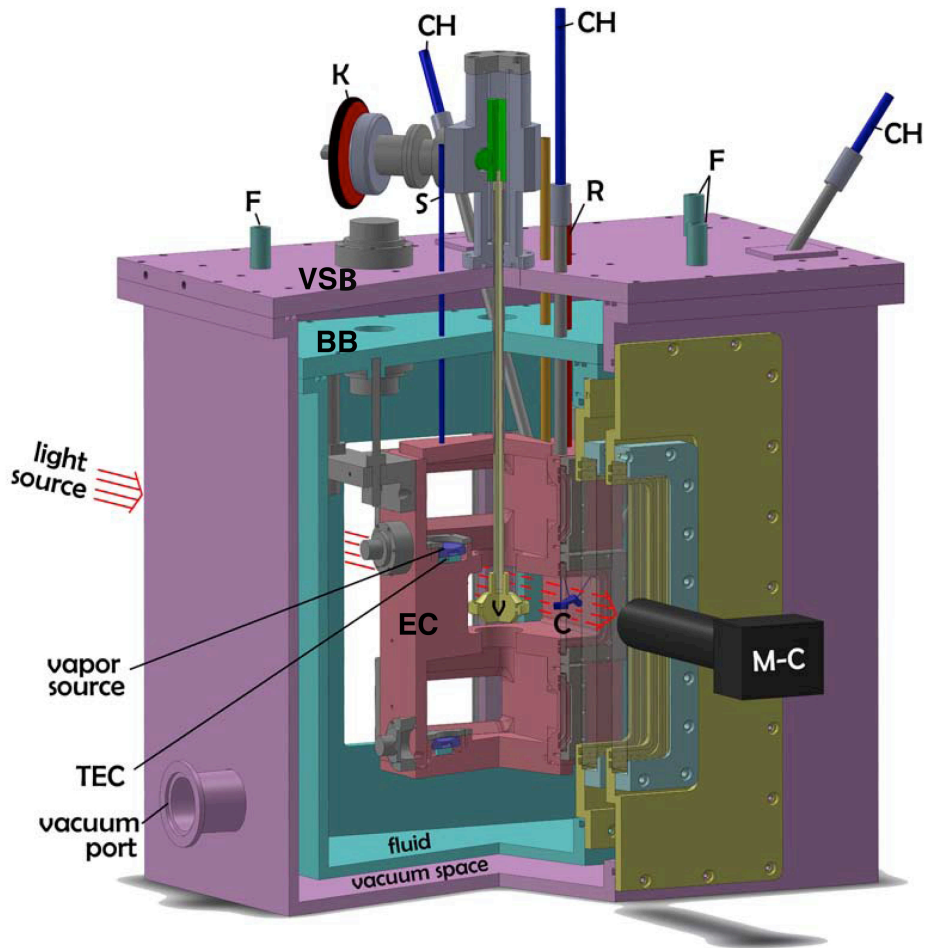


Figure 1. Cut-away of the triple-capillary cryostat (CC2). Both the (turquoise) bath box BB and (purple) vacuum-shroud box VSB surround the (red) experimental chamber EC. The growth chamber GC is the middle chamber in the EC where the crystals C are located. The top and bottom chambers are the two vapor-source chambers VSC each containing a vapor source VS situated on a thermoelectric cooler TEC. The setting of sliding valve V determines which VS sets the humidity in the GC. Other features are CH = capillary holders, F = cryogenic-fluid tubing, K = knob for sliding valve, S and R = tubing for filling vapor-source holders and for monitoring VSC pressure, and MC = SLR camera with telemicroscopic lens. Three sets of silica windows separate the laboratory air and the inside of the GC. For dimensions, the EC is 7" high and the CH tubes are 0.25" diameter.

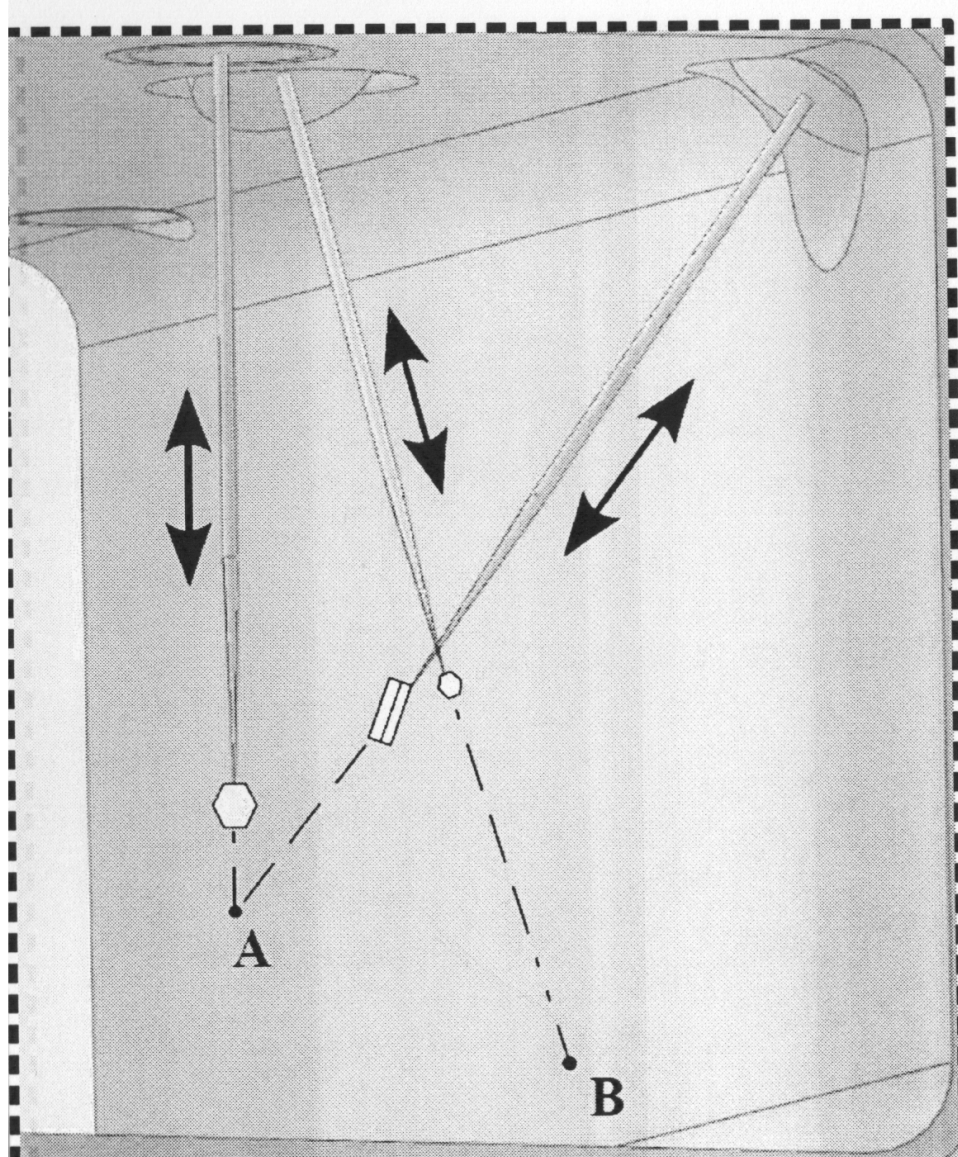


Figure 2. The three capillaries inside the growth chamber (GC) with ice crystals growing at their tips. From left, they are the front capillary Cf, the back capillary Cb (extends to point B on the front window), and the right capillary Cr (intersects with Cf at point A). Capillaries are positioned at center of the GC, [typically with their ends within a 1 cc volume](#), and each capillary can be translated in and out or rotated 36°.

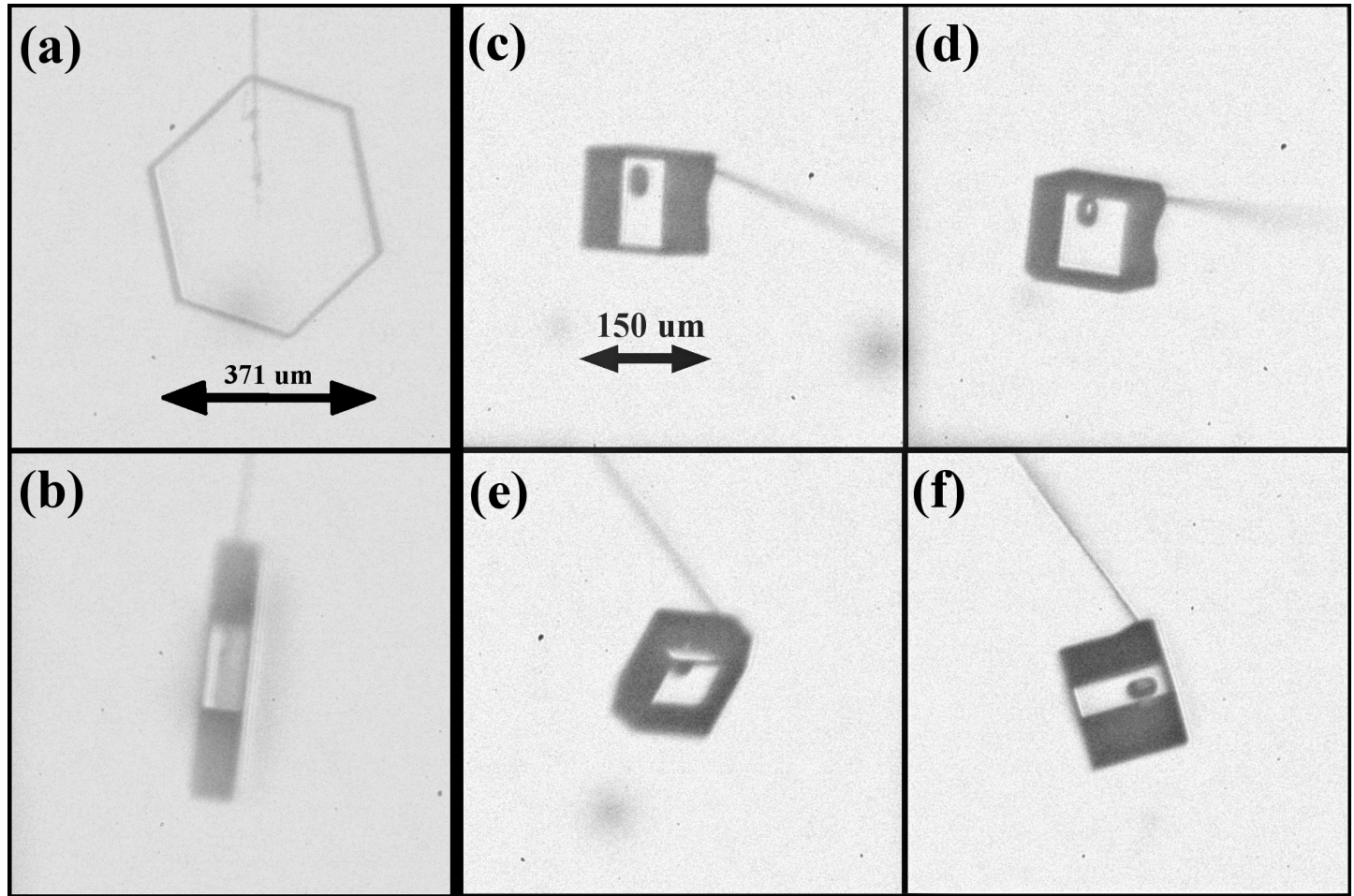


Figure 3. Crystals grown on capillary Cf and Cb. Both crystals nucleated and grew at the same time at -17°C and about 1% supersaturation. a) Cf front view. b) Cf side view. c)-f) are four views of Cb where the difference in capillary direction is due to capillary rotation and the curvature of the capillary.

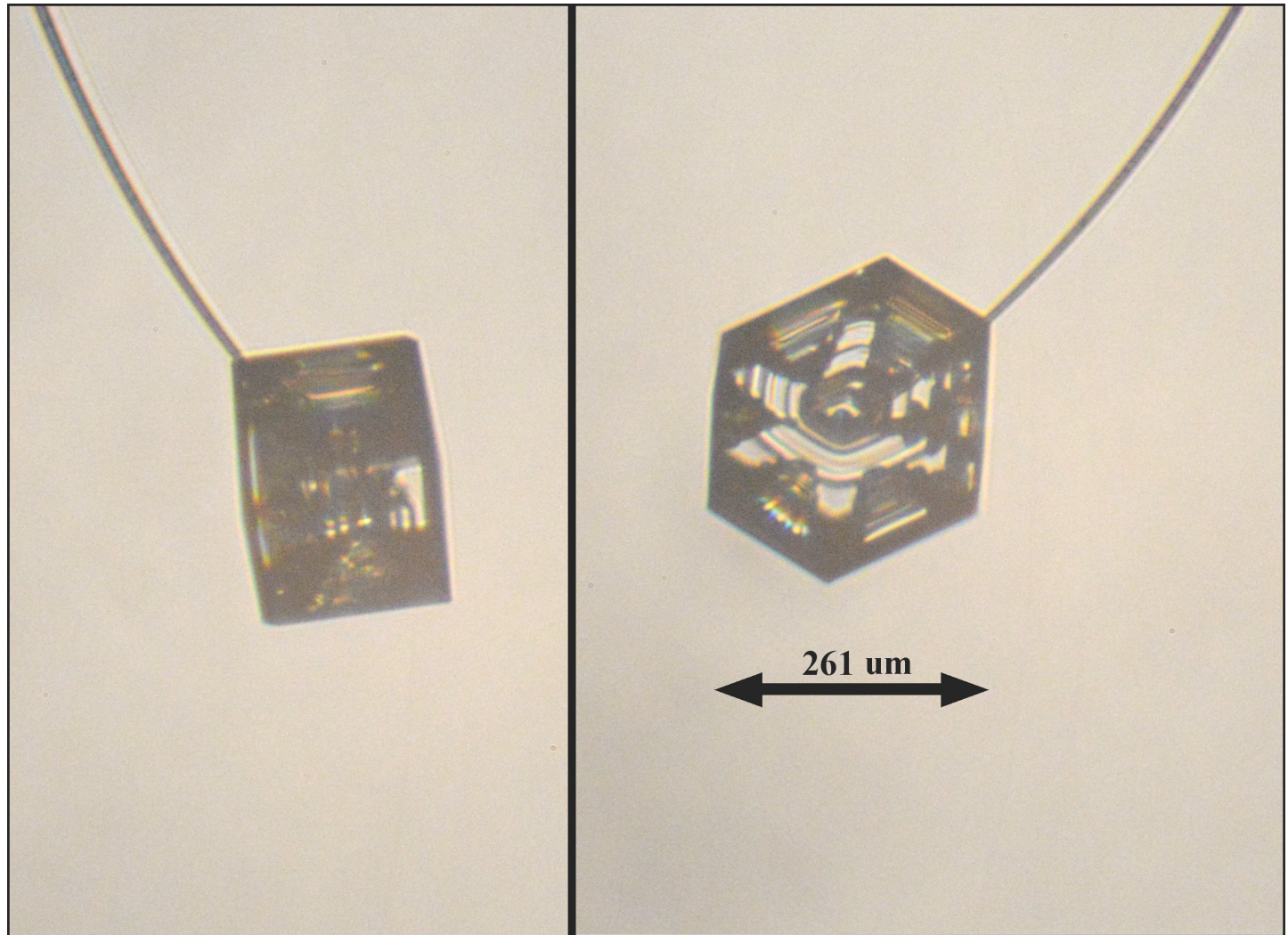


Figure 4. Side and front view of skeletal crystal grown on Cf.

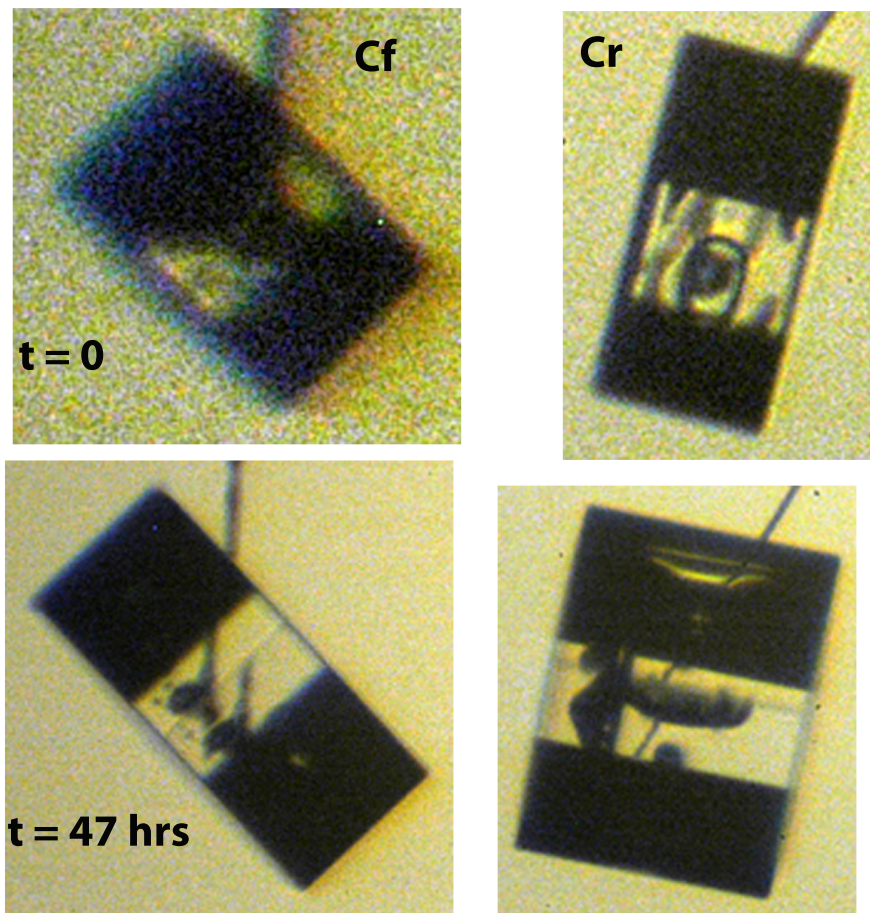


Figure 5. Crystals nucleated from Snomax particles on Cf (left) and Cr (right), grown simultaneously under the same conditions. Top row of images were taken at $t = 0$ and bottom row of images were taken at $t = 47$ hrs. Both crystals have a symmetric prismatic hexagonal shape but developed remarkably different aspect ratios. During part B of the experiment the Cf crystal decreased in aspect ratio while the Cr crystal increased in aspect ratio.

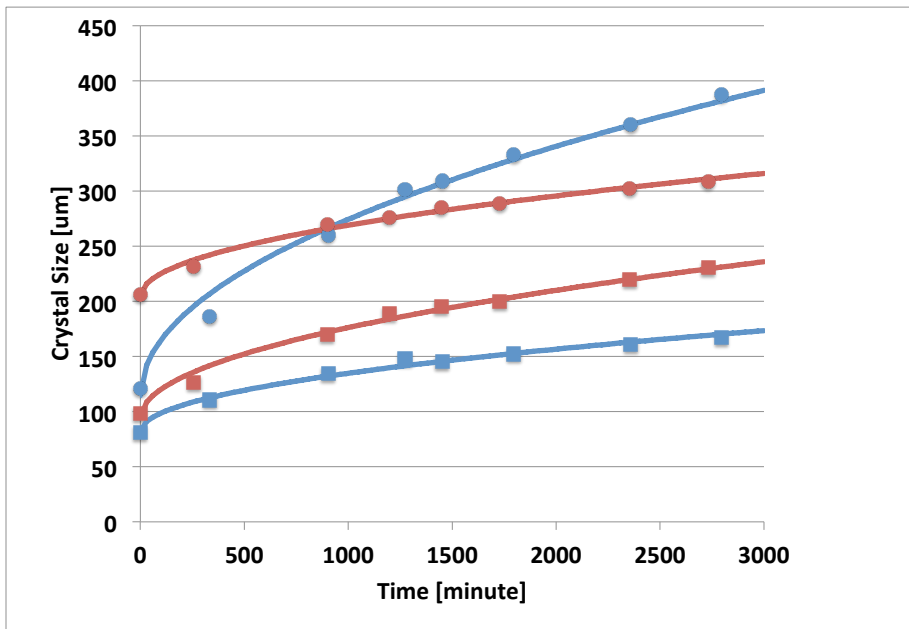


Figure 6. Crystal dimensions $a(t)$ (circles) and $c(t)$ (squares) measured during part B of the experiment for the crystals shown in Fig. 5. Blue points are for the crystal on Cf and the red points are for the crystal on Cr. The lines are the [best-fit](#) for each crystal to a two-parameter power-law parameterization $a(t) = a_0 + g_a * t^{1/2}$ and $c(t) = c_0 + g_c * t^{1/2}$.